wind

MDPI

Article

An Efficient Hybrid Evolutionary Algorithm for Enhanced Wind Energy Capture

Muhammad Rashid [1,*], Abdur Raheem [1,*], Rabia Shakoor [1], Muhammad I. Masud [2], Zeeshan Ahmad Arfeen [1] and Touqeer Ahmed Jumani [3]

[1] Department of Electrical Engineering, Faculty of Engineering & Technology, The Islamia University of Bahawalpur, Bahawalpur 63100, Punjab, Pakistan
[2] Department of Electrical Engineering, College of Engineering, University of Business and Technology, Jeddah 21361, Saudi Arabia
[3] College of Engineering, A'Sharqiyah University, Ibra 400, Oman
* Correspondence: engr.rashid@iub.edu.pk (M.R.); abdur.raheem@iub.edu.pk (A.R.)

Abstract

An optimal topographical arrangement of wind turbines (WTs) is essential for increasing the total power production of a wind farm (WF). This work introduces PSO-GA, a newly formulated algorithm based on the hybrid of Particle Swarm Optimization (PSO) and the Genetic Algorithm (GA) method, to provide the best possible and reliable WF layout (WFL) for enhanced output power. Because GA improves on PSO-found solutions while PSO investigates several regions; therefore, hybrid PSO-GA can effectively handle issues involving multiple local optima. In the first phase of the framework, PSO improves the original variables; in the second phase, the variables are changed for improved fitness. The goal function takes into account both the power production of the WF and the cost per power while analyzing the wake loss using the Jenson wake model. To evaluate the robustness of this strategy, three case studies are analyzed. The algorithm identifies the best possible position of turbines and strictly complies with industry-standard separation distances to prevent extreme wake interference. This comparative study on the past layout improvement process models demonstrates that the proposed hybrid algorithm enhanced performance with a significant power improvement of 0.03–0.04% and a 24–27.3% reduction in wake loss. The above findings indicate that the proposed PSO-GA can be better than the other innovative methods, especially in the aspects of quality and consistency of the solution.

Keywords: hybrid PSO-GA algorithm; metaheuristics optimization; renewable energy; wake effect mitigation; wind farm layout optimization; wind turbine placement

Check for updates

Academic Editors: Pablo Jaen Sola and Erkan Oterkus

Received: 11 December 2025
Revised: 20 January 2026
Accepted: 27 January 2026
Published: 29 January 2026

Copyright: © 2026 by the authors. Licensee MDPI, Basel, Switzerland. This article is an open access article distributed under the terms and conditions of the Creative Commons Attribution (CC BY) license.

1. Introduction

Figure 1 illustrates how the share of renewable power production in the world's power generation has been steadily increasing due to record-breaking new solar and wind system construction. In 2022, solar and wind power accounted for 14% of the world's electrical power production over a given period; the Statistical Review of World Energy 2023 also provides this information. As a result, expanding the usage of renewable energy sources has gained popularity [1].

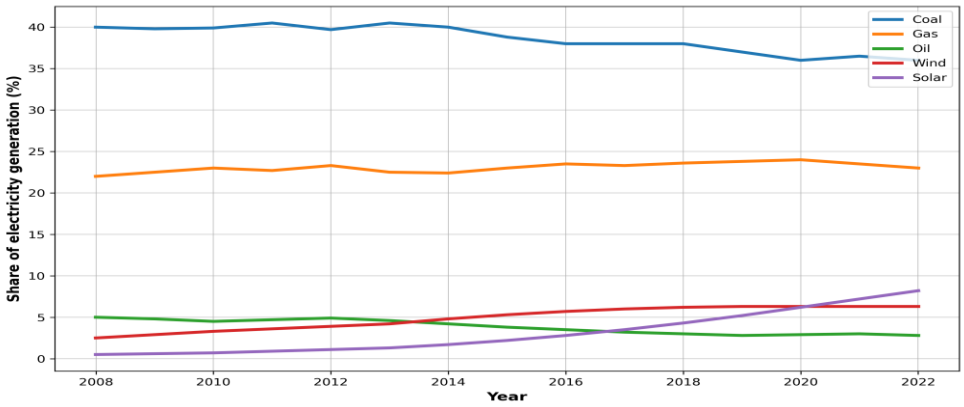


Figure 1. Share of electricity generation by energy source type [1].

At present, wind energy is among the most familiar clean and sustainable sources of electricity in the entire world. As the world desperately requires a means to curtail climate change and reliance on fossil fuels [2], wind energy is increasingly playing an important role in the global transition to renewable Energy [3]. According to a 2021 report by GWEC (Global Wind Energy Council), currently, wind energy represents the second-largest renewable energy source, and its role, according to the projections, will grow to 25 percent of overall non-conventional energy by 2035 [4].

It gets more difficult to develop a WF as the number of turbines increases, since their area grows in proportion to their number. Consequently, there has been a marked shift in emphasis toward curtailing the cost of electricity production, optimizing the architecture of wind farms, and making the most efficient use of wind energy [5]. The WF layout improvement process challenge is nonlinear and constrained, and it relies on multiple variables. A poorly designed wind turbine (WT) layout will counteract the operation and negatively impact the WT wake effect [6]. The accurate simulation of the wake effect is one of the most computationally challenging problems in the improvement process challenge. There have been a number of WF layouts planned recently for enhanced electrical production while minimizing the wake losses.

The nonlinear wake boundary was taken into assessment when Frandsen et al. [7] updated the Jensen wake model [8]. Additionally, by taking into account the basic wind environments in terms of energy expenditure, Mittal and Mitra [9] used the Jensen wake model for the best possible wind farm (WF). Furthermore, using a new goal function, Şişbot et al. [10] replicated the Jensen wake model with comparable findings and improved energy cost findings. Long and Zhang [11] proposed a WF layout design concept based on Cartesian coordinates and a two-echelon grid. A new systematic model based on Yang et al.'s Gaussian wake model was employed by Bastankhah and Porté-Agel [12]. The Park wake model was employed by Yang et al. [13], the two-dimensional Jensen–Gaussian wake model was employed by Gao et al. [14], and Sun et al. [15] used 3D analytical wake models to represent wake deficit. While any of the models can be used to calculate energy produced by the WF, In contrast to the other models, because of its ease of use and ability to compute the energy yield in the shortest time, the Jensen model is the most popular model for WFLO. The study by Pérez, Mínguez [16] and Wu and Porté-Agel [17] asserted that for evaluating energy yields, the Jensen model works better. For this reason, the Jensen wake model was employed in this study. The range of improvement process that considers the interplay between the wakes of different turbines determines the placement of turbines in a WF. The Jensen wake model represents wake expansion and velocity deficit as functions of downstream distance and thrust coefficient. The aerodynamic influence of blade geometry is incorporated implicitly through the thrust coefficient, which captures the integrated effect

of rotor–flow interaction without resolving blade-level aerodynamics. While blade-resolved aerodynamic features are not modeled explicitly, their primary influence on wake strength and wake expansion is embedded within the thrust-based formulation of the Jensen model. This paper provides an efficient hybrid evolutionary method of design integrated with Jensen's model to improve wind farm layouts, considering wake interaction effects, aiming to maximize electrical energy capture.

2. Literature Review

Most of the scholars have utilized metaheuristic methods (MHMs) to tackle the challenges of WF layout (WFL). Mosetti et al. [18] presented a method for optimizing big wind farms with the goal of extracting the most energy for the lowest installation cost. In order to extend production capacity while minimizing the number of installed turbines and the amount of area engaged, Grady et al. [19] used a genetic algorithm strategy to determine the best location for WTs. A process for the best positioning and configuration of WTs within a WF was presented by Marmidis et al. [20] based on the Monte Carlo simulation method. A Monte Carlo-like random search procedural approach was used by Sood et al. [21] to discover the best location for several WTs in a small WF under various wake effects.

Another significant move in the proper improvement process of wind farms, which can possibly enhance the efficiency and effectiveness of wind energy production steps, is that of Masoudi and Baneshi [22]. To find the target goals, Boersma et al. [23] proposed their model, which is a combination of a gradient-based improvement process and evolutionary algorithms. They recommended that the fatigue load can be accommodated by this model, maximum energy can be produced, and the proposed model can additionally provide frequency control. Sun et al. [24] carried out research to optimize wind turbine design and location to achieve maximum energy production with minimum effect on the environment. The aim of the study was to assess how local wind speed acceleration influences the average wind speed at the rotor plane of each wind turbine. Tang et al. [25] explained that by optimizing the placement and operation of turbines, turbine cooperation helps to maximize the energy output of wind farms and reduce their impact on the environment and local communities.

Shakoor et al. [26] formulated a new area rotation scheme to regulate the orientation and dimensions of a WF layout. They formulated a new method to place the turbines in such a way as to maximize their output while also providing sufficient space between adjacent turbines. Stanley et al. [27] demonstrated the effectiveness of their method by applying it to a test case with 16 turbines and two hub heights. They showed that the optimized WF layout with two different hub heights resulted in a 4.7% increase in energy compared to the design with a single hub height. Stanley and Ning [28] presented that a multi-objective improvement process produces more diverse and robust solutions to determine the fatigue damage that a wind turbine's partial waking causes. The suggested arrangement minimizes damage to the farm's turbines while optimizing the WF's yearly energy output. Bouchekara et al. [29] formulated a hybrid model for WTs settlement in a WF in a way that maximizes energy production, minimizes costs, and minimizes environmental impacts. Ramli and Bouchekara [30] demonstrated the Multi-Objective Electric Charged Particles improvement process to produce more diverse and robust solutions, which can lead to significant improvements in WF performance.

It is understandable that there is a gap that needs to be filled by introducing new algorithms to improve the quality of solutions, despite the fact that these significant and varied issues of the WFL-DO challenge have been handled. The phrase "no free lunch" (NFL) is the source of this theory [31]. In accordance with this theory, it is believed that no single MHM is capable of managing all of the improvement process tasks and

identifying the global solutions that work best. It is difficult to develop new algorithms or strategies to enhance existing MHMs for more dynamic handling of complex improvement processes in the NFL. This paper seeks to address the research gap by creating an innovative modified version of Particle Swarm improvement process (PSO) integrated with the Genetic Algorithm (GA), termed PSO-GA, to tackle the WFL-DO challenge. Because GA improves on PSO-based solutions while PSO investigates several regions; therefore hybrid PSO-GA can effectively handle issues involving multiple local optima. In the first phase of the framework, PSO improves the original variables; in the second phase, the variables are changed for improved fitness.

3. Materials and Methods

For a WF to be successful, the WTs must be positioned in the most efficient manner possible. This is because if the turbines are not properly positioned, they may not be able to produce the maximum amount of energy that they are capable of generating. This is due to the wake effect, which can reduce the amount of energy produced by the WF if the turbines are not placed correctly [32]. A square region that is subdivided into Nc identical cells (Nc = 100) is used to analyze the WF that is being studied in this research. Each individual cell measures 5 d by 5 d, where "d" represents the diameter of the turbine. The pivot of each cell is considered to be a potential location for the installation of a wind turbine, with one being the maximum number of turbines that can be placed there, as demonstrated in Figure 2. As a result, to lower the total cost per power unit, the suggested strategy must optimize a WF's turbine arrangement [33]. All simulations were conducted using Python (version 3.11.0, Python Software Foundation, Wilmington, DE, USA) within the Jupyter Notebook environment (version 7.0.2, Project Jupyter). Key libraries used for the simulation included NumPy (version 1.24.3) and SciPy (version 1.10.1).

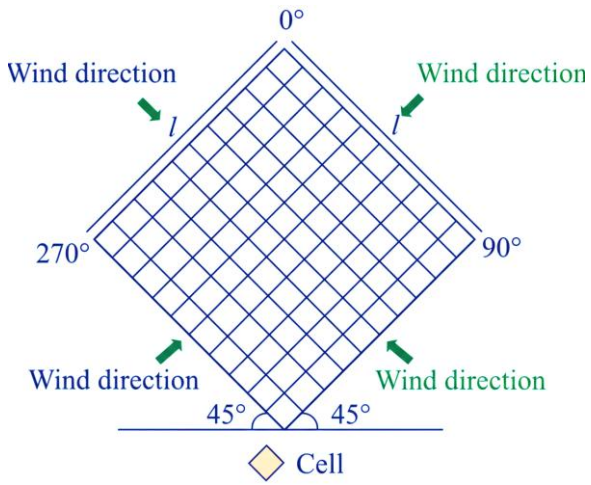


Figure 2. Proposed WF area design.

Three wind speed scenarios, constant wind direction with constant wind speed, variable wind direction with constant wind speed, and variable wind direction with variable wind speed, are used to analyze the suggested hybrid PSO-GA on a multi-objective improvement process challenge (MOP). For the first time, a new version of the Particle Swarm improvement process, known as the PSO-GA method, has been formulated to solve the WFL-DO challenge. The GA strategy is incorporated in hybrid PSO-GA to improve solution quality. The effectiveness of the hybrid PSO-GA procedural approach in comparison to other competing approaches has been confirmed through extensive simulations and com-

parisons to address the multi-objective programming aspects of wind turbine placement issues on conventional land areas.

3.1. Wake Model

It is difficult to predict wake losses in wind farms because of the complex nonlinear dynamics from which they originate. First, a variety of climatic, aerodynamic, and control factors affect how quickly wind strikes a turbine's blades and starts their motion. These factors include wind speed, turbulence level, the aerodynamic properties of the airfoil adopted for the blades, and the pitch angle of each blade separately. Each turbine model operates at its optimal tip-speed ratio, considering all phases of nonlinear friction loss. Recent experimental and computational fluid dynamics investigations have yielded significant insights into turbine–flow interaction and wake formation. For example, Ghamati et al. [34] examined flow interaction effects on turbine performance both experimentally and statistically, providing pertinent insights into wake behavior that validate the modeling assumptions used in this investigation. Power is produced by a rotor driving a gearbox and a final generator. Simultaneously, the airflow leaving the turbine has a lower velocity than the incoming flow. Additionally, turbulence is created when turbine blades rotate, and its intensity can change depending on a number of factors, including the turbine's yaw angle, initial wind speed, turbulence intensity, and blade rotation speed. The resulting wakes expand and interact both vertically and horizontally, and their evolution over time is influenced by complex atmospheric and turbine–wake interactions. Because of this complexity, it is challenging to accurately predict wake behavior, and in order to accurately estimate wake-induced power losses, practical wake models rely on strong hypotheses and simplifying assumptions.

The wake generated by an upstream wind turbine system reduces the effective wind speed and increases turbulence intensity experienced by downstream turbines within the wind farm, leading to a reduction in their power output. Figure 3 illustrates the wake created behind a single wind turbine. As wind with free-stream velocity strikes the rotor, part of its kinetic energy is extracted to produce power. This extraction slows the airflow immediately behind the rotor, creating a region of reduced velocity. The wake gradually expands downstream due to turbulence and mixing with the surrounding air, and its radius grows linearly with distance. Equation (4) shows that the wake radius increases from the reference rotor radius, where α is the axial induction factor, and it is estimated from the thrust coefficient given in Equation (3). The shaded region, therefore, represents the zone of disturbed airflow extending downstream of the turbine. Equation (1) depicts that if there is no wake loss, then the downstream velocity of the ith turbine is the same as the free-stream wind velocity.

$$v_i = v_o \tag{1}$$

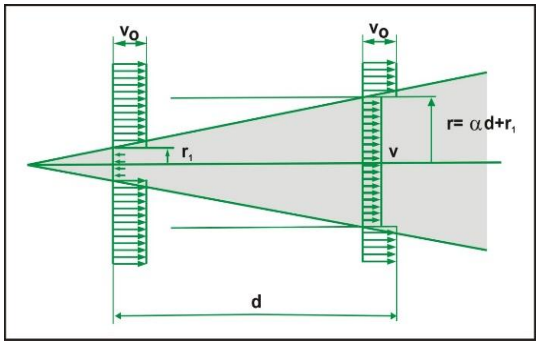


Figure 3. Diagram of the single wake effect model [26].

The Betz limit is used to measure wind speed for the downstream wind turbine, as mentioned in Equation (2).

$$v = v_o \left[1 - \frac{2a}{1 + \left(\frac{\alpha d}{r} \right)^2} \right] \tag{2}$$

where r represents the wake radius at a distance of d behind the turbine

$$C_T = 4a(1 - a) \tag{3}$$

The wake radius r can be calculated from Equation (4).

$$r = \alpha d + r_1 \tag{4}$$

r_1 is called the downstream radius of the wind turbine and can be measured by Equation (5), with r being the rotor radius.

$$r_1 = r\sqrt{\frac{1 - a}{1 - 2a}} \tag{5}$$

$$\alpha = \frac{0.5}{\ln\left(\frac{Z}{Z_o} \right)} \tag{6}$$

The wind speed that a turbine experiences when its wake is not completely formed is known as the partial wake wind speed. The wind speed in this area, which is nearer to the upstream turbine, may change. It takes into account the wake model and how the wake only partially covers the rotor area of the downstream turbine, which slows down the wind relative to the undisturbed flow.

$$v = v_o \left[1 - \frac{2a}{1 + \left(\frac{\alpha d}{r_1} \right)^2} \right] \frac{A_{T,wake,i}}{A_{T,total,i}} \tag{7}$$

$A_{T,wake,i}$ is the wake-affected area of the ith turbine,

$A_{T,total,i}$ is the total area covered by the rotor of the ith turbine.

Wake effects are only due to upstream WTs effects, not to downstream units in the final scenario [35]. For example, the resultant v is represented as follows when numerous full wake effects (apart from partial wake effects) occurring on the ith WT are taken into account.

$$v = v_o \left[1 - \sqrt{\sum_{j=1}^{m_i} 1 - \frac{2a}{1 + \left(\frac{\alpha d}{r_1} \right)^2}} \right]_j \tag{8}$$

m_i denotes the quantity of WTs under wake loss.

Figure 4 demonstrates how wakes behave in a WF with several turbines placed in rows. As upstream turbines generate wakes, downstream turbines are forced to operate in airflows with reduced velocity and higher turbulence. Each turbine in the array, therefore, experiences different inflow conditions depending on its position relative to the wakes created by others. This overlap or 'multi-wake effect' results in a 220% reduction in energy yield and efficiency for downstream turbines. The figure also demonstrates the spacing between turbines, which is a critical design factor; larger spacing helps minimize wake overlap but requires more land, while tighter spacing increases wake losses.

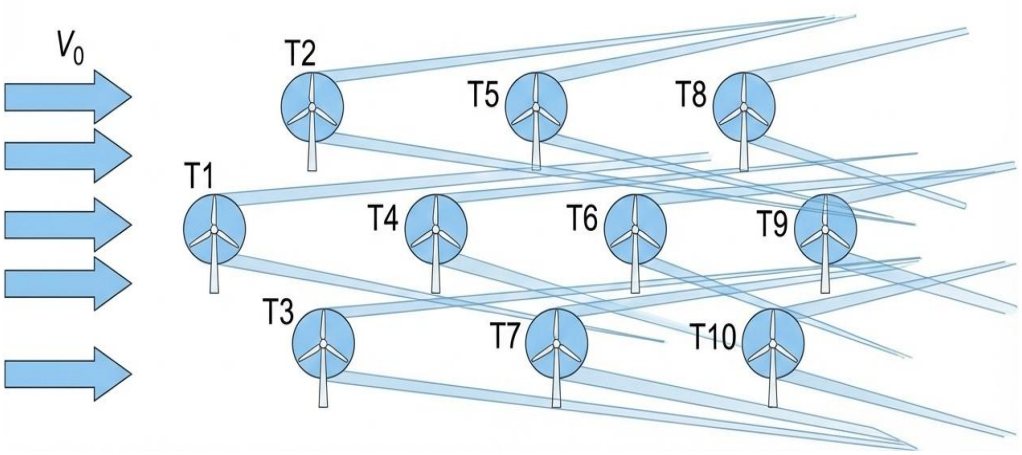


Figure 4. Wake effect of multiple WTs [2].

The Jensen wake model is a popular choice for optimizing the layout of wind farms since it is quick to compute; however, it does not take into consideration the atmospheric stability, complicated turbulence patterns, or far-wake recovery. Despite these drawbacks, the model's balance between computational tractability and accuracy makes it appropriate for comparative optimization research.

3.2. Power Model

A wind turbine's energy yield (P_{wt}) depends on several variables. Total electrical power (available) by the turbine is measured from Equation (9) [36].

$$\text{Electrical Power} = \frac{1}{2}\rho * \pi * r^2 * v^3 * C_p \tag{9}$$

where ρ is the air density, v is the wind velocity, r is the rotor radius, and C_p is the power coefficient. Downstream power taken out from the turbine is measured by the following Equation (10) [36,37].

$$P_{wt} = 0.3V^3 \tag{10}$$

where v is the downstream wind velocity. The constant coefficient 0.3 represents a lumped normalization factor obtained by assuming standard air density, a fixed rotor swept area, and an average power coefficient C_p.

Total available electrical power taken out from the turbine is measured by the following Equation (11).

$$P_{wt} = 0.3{V_0}^3 \tag{11}$$

where V_0 is the free-stream wind velocity.

The following Equation (12) determines the cut-in, cut-out, rated wind speeds, and associated output power for each WT, as shown in Figure 5.

$$P_{wt}\,(V) = \begin{Bmatrix} 0 & \text{if } V < V_{Cut-in} \\ 0.3V^3 & V_{Cut-in} \le V < V_{rated} \\ 518.4\text{ KW} & \text{if } V_{rated} < V \le V_{Cut-out} \\ 0 & V > V_{Cut-out} \end{Bmatrix} \tag{12}$$

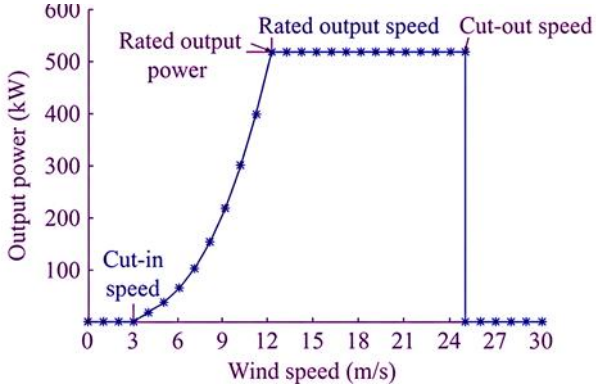


Figure 5. Output power curve for WT [38].

3.3. Cost Model

The cost of the whole WF is measured by (13) [39].

$$\text{Cost} = \text{N}\left(\frac{2}{3} + \frac{1}{3}\text{e}^{-0.00174\text{N}^2}\right) \tag{13}$$

where N is the total number of WTs.

3.4. Objective Function

The objective functions of this study are as follows.

$$\text{Objective} = \text{Minimize}\left[1 - \frac{2\text{a}}{1 + \left(\frac{\alpha\text{d}}{\text{r}}\right)^2}\right] \tag{14}$$

$$\text{Objective} = \text{Minimize}\,\frac{\text{Cost}}{\text{Electrical Power}} \tag{15}$$

3.5. Constraints Modeling

The first restriction that needs to be taken into account is that every wind turbine needs to be situated on the land where the WF is intended to be constructed. This restriction can be stated as follows:

$$\text{x}_{\text{min}} \leq \text{x}_\text{i} \leq \text{x}_{\text{max}}$$

$$\text{y}_{\text{min}} \leq \text{y}_\text{i} \leq \text{y}_{\text{max}}\ \text{i} = 1:\text{n}$$

Another constraint to be considered is that two nearby WTs must be within a distance limit. The following is a mathematical formulation of this limitation.

$$\sqrt{\left(\text{x}_\text{i} - \text{x}_\text{j}\right)^2 - \left(\text{y}_\text{i} - \text{y}_\text{j}\right)^2} \geq \text{D}_{\text{min}} \qquad \text{i} = 1:\text{n}$$

In this study, the y-axis distance is chosen to be eight times the wind turbine's rotor radius.

3.6. Energy Efficiency Index (EEI)

The EEI is the effectiveness with which a wind farm design transforms available land area into usable electrical power.

$$\text{EEI} = \frac{\text{Power Generated}}{\textit{Land Used}} \times \eta \tag{16}$$

The term η accounts for the combined effects of losses occurring in the turbine–generator system.

3.7. Particle Swarm Improvement Process (PSO) Algorithm

Particle Swarm improvement process (PSO) is a computer-based strategy for solving challenging problems where we must identify the most desirable solution among a large number of options available to us. PSO is based on the flight behavior of birds in flocks or fish in schools. And when a bunch of birds are seeking food, no one knows the exact location of the food. But by testing one after another and improving by observing the best position that has been discovered to date, they finally get to the food. The same concept is employed by PSO to find the answers to mathematics and engineering problems [40].

In PSO, the algorithm treats every possible solution as a particle, and together, these particles form a swarm searching for the best result. In the Particle Swarm Optimization, each particle is characterized by both position and velocity, where the position represents the candidate solution at a given iteration, as given in Equation (17).

$$X_{t+1}^{i} = X_{t}^{i} + V_{o}(t+1) \tag{17}$$

where X represents the turbine position.

Velocity reflects the direction and pace at which it will progress towards a superior solution. In the search, every particle recalls.

$$v_{o}(t+1) = \varpi v_{o}(t) + C_1R_1 \odot (\mathbb{P}^{p}(x) - \mathbb{P}(x)) + C_2R_2 \odot \left(\mathbb{P}^{\}}(x) - \mathbb{P}(x)\right) \tag{18}$$

ϖ = Inertia weight, $\mathbb{P}^{p}$ = Particle best position, $\mathbb{P}^{\}}(x)$ = Global best position, R_1 R_2 = random variables, v_o = Free-stream wind velocity.

Figure 6a represents the flow chart of the PSO algorithm:

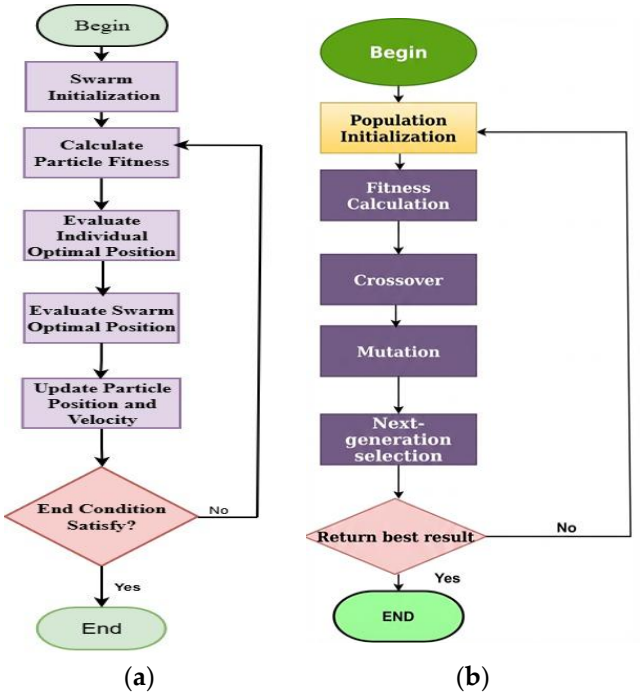
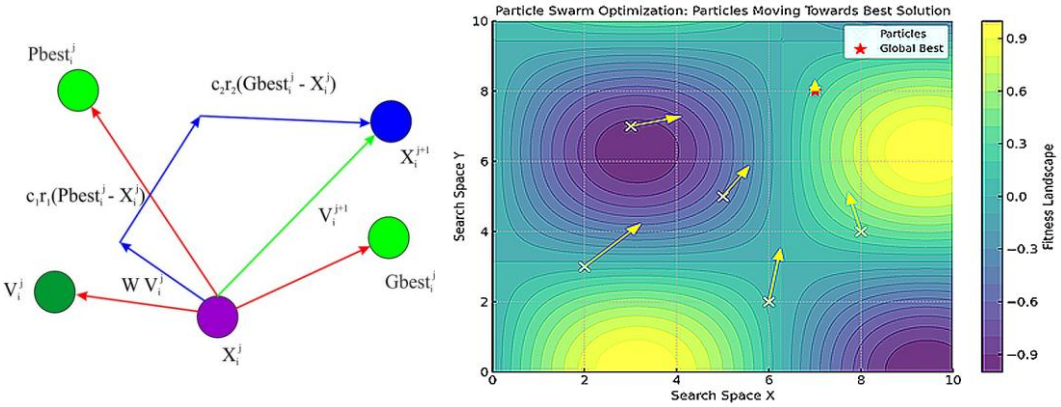


Figure 6. Flow charts: (**a**) flow chart of Particle Swarm improvement process algorithm; (**b**) flow chart of Genetic Algorithm.

The iteration procedure of any particle in each generation is illustrated in Figure 7a,b. The optimized particle shown in Figure 7b, therefore, represents a stable convergence outcome rather than a stochastic artifact. A sociological analysis of the velocity update formula reveals that the influence of the particle's prior velocity is the first component of this updated formula (Equation (18)). Because it demonstrates that the particle performs inertial motion in accordance with its own velocity and has confidence in its current moving state, the parameter ω is referred to as the inertia weight. The distance between the particle's current location and its ideal location determines the second component, often known as the "cognitive" item. It refers to the particle's own reasoning, that is, the movement brought about by its own experiences [38].



(**a**) (**b**)

Figure 7. Iteration procedure of any particle: (**a**) particle movement along with the PSO algorithm's updating of location and velocity, and (**b**) conceptual diagram of PSO.

3.8. Genetic Algorithm (GA)

According to El-Shorbagy and El-Refaey [41], the GA is an appropriate tool for addressing improvement process problems that involve a large number of variables and limitations. The Genetic Algorithm (GA) is a population-based improvement process method inspired by the principle of natural selection. It employs genetic operators such as selection, crossover, and mutation to evolve better solutions across generations. A population size of 500, a generation count of 2000, a crossover rate of 0.7, and a mutation rate of 0.02 are used in this study. The GA follows a structured sequence: random initialization, fitness evaluation, parent selection, crossover, mutation, and elitist replacement. Figure 6b presents the flowchart of the GA improvement process.

Genetic Algorithm (GA) involves bio-inspired evolutionary optimization techniques that utilize concepts of natural selection and genetics and has been widely applied in a range of engineering domains as a subset of artificial intelligence-based optimization approaches. It is able to identify the best possible result on a global scale [42].

Simply, a Genetic Algorithm is survival of the fittest, but in computer problems, it can keep trying many solutions until it finds one that works well by simulating the ways that nature has given species advancements throughout time.

3.9. Proposed (PSO-GA) Algorithm

The hybrid PSO-GA method, which combines the global search capability of PSO with the solution refining capabilities of GA, can enhance the turbine placement in the WF layout improvement process. This is especially helpful for complicated improvement process problems with a large search space and several local optima. In order to update the turbine placements, the hybrid algorithm must take into account both the best possible

solution currently determined by PSO and the new solutions produced by GA's crossover and mutation. Turbine layouts produced using this strategy are more resilient and effective and are less likely to deviate from best configurations.

In the suggested hybrid framework, Particle Swarm Optimization (PSO) is initially utilized to investigate the global search space and determine a collection of near-optimal turbine configurations. After that, these PSO-derived solutions are moved to the GA phase, where they serve as the starting population for more improvement. While crossover and mutation operators add controlled variation, elitism is used to maintain the best-performing layouts. Penalizing unfeasible turbine locations that go against minimum separation distances or boundary constraints is how constraint handling is implemented.

Recent improvements in the engineering improvement process have allowed for the move from traditional trial-and-error design techniques to fully automated ones. This is primarily due to the rapid development of metaheuristic search algorithms, which have shown to be efficient and robust when dealing with real-world issues. Many scholars have already investigated the subject of the best possible layout design for wind farms. But still, there is a gap present.

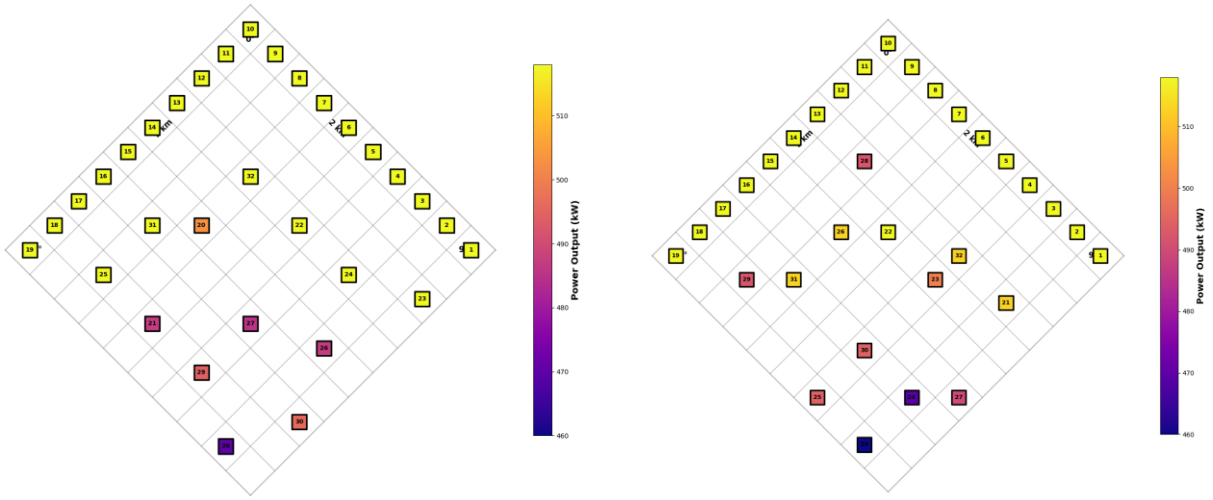
4. Results

The objective of this research was to evaluate the effectiveness of the PSO-GA hybrid algorithm in optimizing the layout of WTs for maximizing the electrical energy yield of a WF while adhering to industry-standard separation distances to avoid wake interference. Through extensive simulation using the proposed framework, the PSO-GA strategy demonstrated significant improvement in both energy yield and cost efficiency of the WF. The case studies analyzed three different WF configurations, each involving a 2 km $\times$ 2 km area subdivided into 100 cells of 200 m $\times$ 200 m. The framework was tested under varying conditions of wind speed and wind turbine alignment with a consistent focus on the minimization of wake interference while maintaining high turbine efficiency and power generation output. PSO algorithm explored a broad search space, effectively navigating through multiple local optima to identify promising candidate solutions. The PSO's ability to adjust the particle positions in the search space using its velocity and acceleration coefficients allowed it to investigate various regions of the WF layout space without getting stuck in suboptimal solutions. The following PSO variables are used for the quick response: the particle restriction variables are inertia weight coefficient = 0.5, acceleration coefficient constants C_1 = 2.5, C_2 = 2.5, and the maximum number of iterations $Iter_{max}$ = 100. A uniform distribution is applied in picking random numbers R_1 and R_2 between 0 and 1.

Once the PSO had determined a near-best possible layout, the GA was used to refine the positions of the turbines, improving the energy yield and further reducing the wake interference. The genetic operators (crossover and mutation) enabled the algorithm to explore variations in turbine positioning, balancing power yield improvement process with the minimization of wake effects. Through the iterative refinement process, the PSO-GA algorithm outperformed standalone PSO and GA algorithms in terms of the total electrical energy yield, with a substantial increase in energy yield over conventional layout configurations. The improvement process ensured that each turbine was placed in a location that maximized its energy capture potential, while also preventing excessive overlap in the wake regions of adjacent turbines.

4.1. Case 1

Figure 8a represents the improved layout obtained through the proposed hybrid PSO-GA approach, while Figure 8b reflects the reference layout used for comparison.



(**a**) (**b**)

Figure 8. Wind farm layout for Case 1: (**a**) proposed method; (**b**) simulated results using the method described by Asaah and Philip in [43].

The optimum configuration produces a maximum power output with 32 turbines working under a uniform inflow wind speed of 12 m/s, as shown in Figure 9a,b. An average turbine efficiency of about 98.8%, the effective wind speed of 11.95 m/s, and individual turbine efficiencies ranging from 98.8% to 100% show that the algorithm converges on a highly efficient configuration. There is little variance in the effective wind speed distribution between 11.62 and 12.00 m/s throughout the farm.

No of Wind Turbines = 32

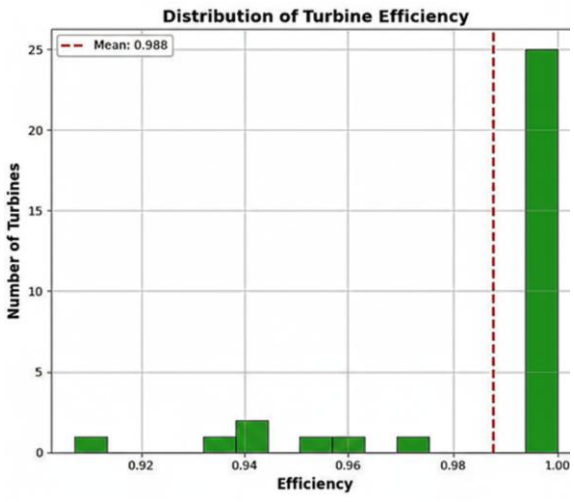
Average Turbine Efficiency = 0.988

Efficiency Range = 0.988–1.000

Wind Turbines with 100% efficiency = 25

Average Effective Wind Speed = 11.95 m/s

Wind Speed Range = 11.62–12.00 m/s



(**a**) (**b**)

Figure 9. (**a**) Summary of wind farm performance parameters for Case 1; (**b**) scattering of the frequency of the proposed study.

Table 1 demonstrates the performance of the proposed layout compared with previous research. The proposed strategy extracts 16,389.73 kW, which is higher than the earlier reported 16,326.55 kW. A major difference appears in wake losses: the proposed configuration records 199.06 units, in place of 262.21 units, indicating that the proposed layout better minimizes wake interactions. Overall, the proposed layout demonstrates

superior optimization by enhancing power capture and reducing wake-induced losses, outperforming the approach presented in [43].

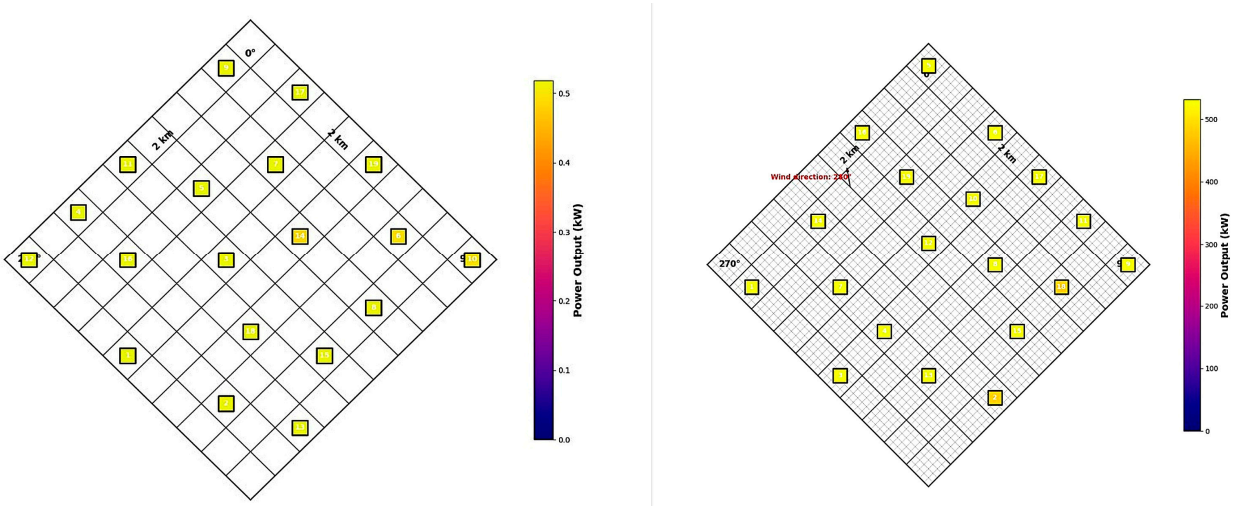
Table 1. Performance Analysis of Case 1.

Strategy	Nt	Power Extracted	Wake Loss	AEP (MWh)	Efficiency %
Proposed	32	16,389.73	199.06	143,574,034.8	98.8
[43]	32	16,326.59	262.2	143,020,928.4	98.42

Efficiency (%) is determined by comparing the net energy generated by the wind farm, accounting for wake interactions, with the theoretical maximum energy that would be produced by an equivalent number of turbines functioning independently under identical wind conditions.

4.2. Case 2

Figure 10a represents the improved layout obtained through the proposed hybrid PSO-GA approach, while Figure 10b reflects the reference layout used for comparison.



(**a**) (**b**)

Figure 10. Wind farm layout for Case 2: (**a**) proposed method; (**b**) simulated results using the method described by Asaah and Philip in [43].

The optimum configuration produces a maximum power output with 19 turbines working under a uniform inflow wind speed of 12 m/s, as shown in Figure 11a,b; with an average turbine efficiency of about 99.2%, the effective wind speed of 11.95 m/s, and individual turbine efficiencies ranging from 94.9% to 100%, the algorithm converges on a highly efficient arrangement. There is little fluctuation in the effective wind speed distribution between 11.76 and 12.00 m/s throughout the farm. The single wind turbine exhibited 100% efficiency, specifically when the wind direction aligned with 310°.

The performance of the proposed layout compared with previous research is shown in Table 2. The suggested method extracts 9770.8 kW, which is marginally more than the 9741.3 kW. Wake loss shows a significant difference: the suggested configuration records 78.7968 units, instead of 108.3 units. This suggests that the proposed structure more effectively reduces wake interactions. Overall, by improving power capture and lowering wake-induced losses, the proposed configuration exhibits improved optimization than the technique existing in [43].

Best Wind Direction =310^{o}

No of Wind Turbines = 19

Average Turbine Efficiency = 0.992

Efficiency Range = 0.949–1.000

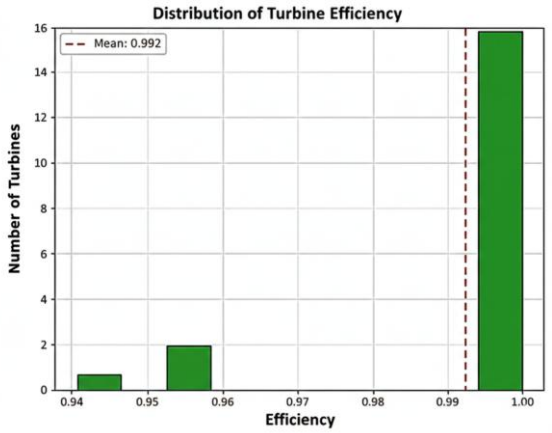
Wind Turbines with 100% efficiency = 16

Reference Wind Speed = 12.00 m/s

Average Effective Wind Speed = 11.97 m/s

Wind Speed Range= 11.76–12.00 m/s

(**a**)



(**b**)

Figure 11. (**a**) Summary of wind farm performance parameters for Case 2; (**b**) scattering of the frequency of the proposed study.

Table 2. Performance Analysis of Case 2.

Strategy	Nt	Power Extracted	Wake Loss	AEP (MWh)	Efficiency %
Proposed	19	9770.8032	78.7968	85,592.2	99.2
[43]	19	9741.3	108.3	85,333.79	98.9

4.3. Case 3

Figure 12 illustrates that the chance of wind speed is higher when the wind direction is between 270° and 350°. The performance of the suggested layout compared with an earlier study is shown in Table 3. The suggested method extracts 7713.79 kW, which is somewhat more than the 7690.46 kW. Wake loss shows a significant difference: the proposed configuration records 62.21 units, instead of 85.54 units, suggesting that the proposed layout more effectively reduces wake interactions. Overall, by improving power capture and lowering wake-induced losses, the proposed layout performs better than the method implemented in [43].

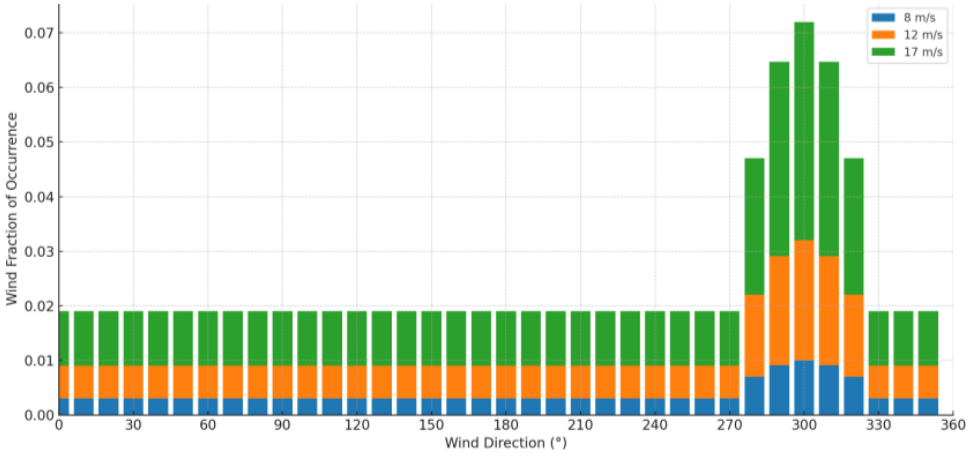


Figure 12. Wind probability in case 3.

Table 3. Performance Analysis of Case 3.

Strategy	Nt	Power Extracted	Wake Loss	AEP (MWh)	Efficiency %
Proposed	15	7713.79	62.21	67,572.8	99.2
[43]	15	7690.46	85.54	67,368.4	98.9

The improvements are almost constant across all test situations and are accompanied by significant reductions in wake losses, despite the fact that the absolute gains in power output appear to be numerically tiny. Even small percentage increases in large-scale wind farms result in substantial long-term energy production and financial gains during the course of operation. Additionally, the suggested approach shows enhanced layout resilience and decreased wake interaction, both of which are essential for the development of large-scale wind farms.

To confirm that the observed enhancements are not mere effects of numerical tolerance or stochastic noise, each optimization scenario was conducted across numerous independent iterations. The given results, which show averaged results, validate the robustness and repeatability of the suggested PSO-GA architecture.

The Energy Efficiency Index (EEI) values for three distinct test cases employing two wind farm layout optimization strategies, the proposed strategy and the reference approach described in the paper [43], are shown in Table 4. The EEI measures the layout's quality for each scenario based on how well the available wind farm area is transformed into electrical power that can be used. Better performance is indicated by higher EEI scores. The paired t-test in Table 4 demonstrates that the improvement is statistically significant and that the proposed strategy consistently produces higher EEI values for each case.

Table 4. Comparison of Energy Efficiency Index (EEI).

Case #	EEI by Proposed Strategy	EEI [43]	*p*-Value
Case 1	4048.26	4016.34	
Case 2	2423.2	2406.1	0.0066
Case 3	1913.01	1899.5	

A paired t-test was utilized to statistically compare the Energy Efficiency Index (EEI) values derived from the proposed strategy and the reference method under identical wind circumstances. Under the assumption that paired differences were normal, each case was assessed throughout several separate optimization runs. The ensuing p-values verify that the noted gains are not random fluctuations but rather statistically significant.

A p-value ≤ 0.01 indicates that the observed improvements are unlikely to have arisen from stochastic variability in the optimization process. Instead, the gains are attributable to the structured hybridization of PSO and GA, which enhances the balance between global exploration and local exploitation. This leads to consistent reductions in wake losses and improved turbine placement geometry across multiple independent runs, resulting in statistically reproducible and physically interpretable performance improvements.

Figure 13 demonstrates that, in comparison to the method applied in [43], the suggested optimization methodology is effective in improving wind farm layout performance.

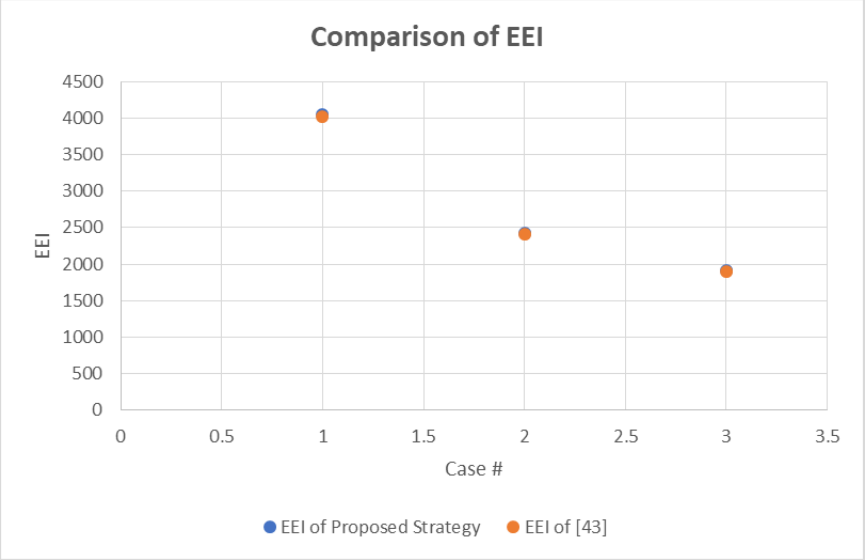


Figure 13. Comparison of EEI results between the proposed method and the method by Asaah et. al. [43].

5. Conclusions

This study presents a novel hybrid optimization technique that successfully combines hybrid PSO-GA with the Jensen wake model to address the WFLO problem in actual wind conditions. Unlike in previous research, this approach incorporates a dynamic goal function that takes into account cost, energy yield, and efficiency by minimizing the wake loss. This paper delineated the optimum WFLOs under three case studies of wind speed and direction. In order to obtain the maximum possible output power, each WT's position was appropriately selected. In summary, the hybrid PSO-GA algorithm provided a very effective method for optimizing wind farm layouts, leading to significant increases in power output and cost effectiveness while preventing severe wake disruption. The algorithm's practical relevance in real-world wind farm design is demonstrated by its robustness across three different case studies and its capacity to manage the trade-off between electricity generation and turbine cost. The suggested PSO-GA significantly reduced wake loss and improved efficiency by 0.4%, 0.3%, and 0.3%, respectively, in the case studies, as compared to existing WFLO techniques. Future work could focus on the algorithm's performance by incorporating advanced techniques such as a multi-objective improvement process to simultaneously optimize for multiple objectives, such as environmental impact and operational costs. Although advances have been noted, it is recognized that these advancements may not always result in significant operational advantages in all real-world scenarios. Wake model assumptions, wind variability, and cost simplifications all affect how applicable the suggested method is. These constraints underscore the potential for expanding the framework to incorporate high-fidelity flow models, uncertainty quantification, and thorough economic evaluations.

Author Contributions: This work presents An Efficient Hybrid Evolutionary Algorithm for Enhanced Wind Energy Capture. M.R., A.R. and R.S. thought of the initial idea. M.R., A.R., R.S. established the methodological strategy. M.R., M.I.M., Z.A.A. and T.A.J. formulated the software component. M.R., A.R., R.S. and T.A.J. oversaw the validation process. M.R., M.I.M., Z.A.A. and T.A.J. provided the resources. M.R. prepared the initial draft. M.R., A.R., R.S., M.I.M., Z.A.A. and T.A.J. contributed to revisions and edits. A.R. and R.S. provided overall supervision. All authors have read and agreed to the published version of the manuscript.

Funding: This research received no external funding.

Institutional Review Board Statement: Not applicable.

Informed Consent Statement: Not applicable.

Data Availability Statement: The data presented in this study are available on request from the corresponding authors.

Conflicts of Interest: The authors declare no conflicts of interest.

Nomenclature

The following nomenclatures are used in this manuscript:

EEI	Energy Efficiency Index
GA	Genetic Algorithm
GWEC	Global Wind Energy Council
MHMs	Metaheuristic Methods
MOP	Multi-Objective Improvement Process
NFL	No Free Lunch
PSO	Particle Swarm Optimization
WF	Wind Farm
WFL	Wind Farm Layout
WFLO	Wind Farm Layout Optimization
WFL-DO	Wind Farm Discrete Optimization
WT	Wind Turbine
ρ	Air Density
α	Axial Induction Factor
π	Pi
η	Efficiency
C_p	Power Coefficient
C_T	Thrust Coefficient
ϖ	Inertia Weight
$\mathbb{P}^{\mathfrak{p}}$	Particle Best Position
$\mathbb{P}^{\}}(x)$	Global Best Position

References

1. Yu, X.; Zhang, W. A teaching-learning-based optimization algorithm with reinforcement learning to address wind farm layout optimization problem. *Appl. Soft Comput.* **2024**, *151*, 111135. [CrossRef]
2. Xiong, L.; Liu, X.; Liu, Y.; Zhuo, F. Modeling and stability issues of voltage-source converter-dominated power systems: A review. *CSEE J. Power Energy Syst.* **2020**, *8*, 1530–1549.
3. Wang, L.; Dong, M.; Yang, J.; Wang, L.; Chen, S.; Duić, N.; Joo, Y.H.; Song, D. Wind turbine wakes modeling and applications: Past, present, and future. *Ocean Eng.* **2024**, *309*, 118508. [CrossRef]
4. Roga, S.; Bardhan, S.; Kumar, Y.; Dubey, S.K. Recent technology and challenges of wind energy generation: A review. *Sustain. Energy Technol. Assess.* **2022**, *52*, 102239.
5. Hou, P.; Hu, W.; Soltani, M.; Chen, Z. Optimized placement of wind turbines in large-scale offshore wind farm using particle swarm optimization algorithm. *IEEE Trans. Sustain. Energy* **2015**, *6*, 1272–1282. [CrossRef]
6. Abdelsalam, A.M.; El-Shorbagy, M.A. Optimization of wind turbines siting in a wind farm using genetic algorithm based local search. *Renew. Energy* **2018**, *123*, 748–755. [CrossRef]
7. Frandsen, S.; Barthelmie, R.; Pryor, S.; Rathmann, O.; Larsen, S.; Højstrup, J.; Thøgersen, M. Analytical modelling of wind speed deficit in large offshore wind farms. *Wind Energy* **2006**, *9*, 39–53. [CrossRef]
8. Barthelmie, R.J.; Rathmann, O.; Frandsen, S.T.; Hansen, K.S.; Politis, E.; Prospathopoulos, J.; Rados, K.; Cabezón, D.; Schlez, W.; Phillips, J.; et al. Modelling and measurements of wakes in large wind farms. *J. Phys. Conf. Ser.* **2007**, *75*, 012049. [CrossRef]
9. Mittal, P.; Mitra, K. Determining layout of a wind farm with optimal number of turbines: A decomposition based approach. *J. Clean. Prod.* **2018**, *202*, 342–359. [CrossRef]
10. Şişbot, S.; Turgut, Ö.; Tunç, M.; Çamdalı, Ü. Optimal positioning of wind turbines on Gökçeada using multi-objective genetic algorithm. *Wind Energy Int. J. Prog. Appl. Wind Power Convers. Technol.* **2010**, *13*, 297–306. [CrossRef]
11. Long, H.; Zhang, Z. A two-echelon wind farm layout planning model. *IEEE Trans. Sustain. Energy* **2015**, *6*, 863–871. [CrossRef]

12. Bastankhah, M.; Porté-Agel, F. A new analytical model for wind-turbine wakes. *Renew. Energy* **2014**, *70*, 116–123. [CrossRef]
13. Yang, Q.; Hu, J.; Law, S.-S. Optimization of wind farm layout with modified genetic algorithm based on boolean code. *J. Wind Eng. Ind. Aerodyn.* **2018**, *181*, 61–68.
14. Gao, X.; Yang, H.; Lu, L. Optimization of wind turbine layout position in a wind farm using a newly-developed two-dimensional wake model. *Appl. Energy* **2016**, *174*, 192–200. [CrossRef]
15. Sun, H.; Gao, X.; Yang, H. A review of full-scale wind-field measurements of the wind-turbine wake effect and a measurement of the wake-interaction effect. *Renew. Sustain. Energy Rev.* **2020**, *132*, 110042. [CrossRef]
16. Pérez, B.; Mínguez, R.; Guanche, R. Offshore wind farm layout optimization using mathematical programming techniques. *Renew. Energy* **2013**, *53*, 389–399. [CrossRef]
17. Wu, Y.-T.; Porté-Agel, F. Simulation of turbulent flow inside and above wind farms: Model validation and layout effects. *Bound.-Layer Meteorol.* **2013**, *146*, 181–205. [CrossRef]
18. Mosetti, G.; Poloni, C.; Diviacco, B. Optimization of wind turbine positioning in large windfarms by means of a genetic algorithm. *J. Wind Eng. Ind. Aerodyn.* **1994**, *51*, 105–116.
19. Grady, S.A.; Hussaini, M.Y.; Abdullah, M.M. Placement of wind turbines using genetic algorithms. *Renew. Energy* **2005**, *30*, 259–270. [CrossRef]
20. Marmidis, G.; Lazarou, S.; Pyrgioti, E. Optimal placement of wind turbines in a wind park using Monte Carlo simulation. *Renew. Energy* **2008**, *33*, 1455–1460. [CrossRef]
21. Sood, P.; Winstead, V.; Steevens, P. Optimal placement of wind turbines: A Monte Carlo approach with large historical data set. In Proceedings of the 2010 IEEE International Conference on Electro/Information Technology, Normal, IL, USA, 20–22 January 2010.
22. Masoudi, S.M.; Baneshi, M. Layout optimization of a wind farm considering grids of various resolutions, wake effect, and realistic wind speed and wind direction data: A techno-economic assessment. *Energy* **2022**, *244*, 123188. [CrossRef]
23. Boersma, S.; Doekemeijer, B.; Vali, M.; Meyers, J.; van Wingerden, J.W. A control-oriented dynamic wind farm model: WFSim. *Wind Energy Sci.* **2018**, *3*, 75–95. [CrossRef]
24. Sun, H.; Qiu, C.; Lu, L.; Gao, X.; Chen, J.; Yang, H. Wind turbine power modelling and optimization using artificial neural network with wind field experimental data. *Appl. Energy* **2020**, *280*, 115880. [CrossRef]
25. Tang, X.Y.; Yang, Q.; Stoevesandt, B.; Sun, Y. Optimization of wind farm layout with optimum coordination of turbine cooperations. *Comput. Ind. Eng.* **2022**, *164*, 107880. [CrossRef]
26. Shakoor, R.; Hassan, M.Y.; Raheem, A.; Rasheed, N. Wind farm layout optimization using area dimensions and definite point selection techniques. *Renew. Energy* **2016**, *88*, 154–163. [CrossRef]
27. Stanley, A.P.J.; Ning, A.; Dykes, K. Optimization of turbine design in wind farms with multiple hub heights, using exact analytic gradients and structural constraints. *Wind Energy* **2019**, *22*, 605–619. [CrossRef]
28. Stanley, A.P.; Ning, A. Coupled wind turbine design and layout optimization with nonhomogeneous wind turbines. *Wind Energy Sci.* **2019**, *4*, 99–114.
29. Bouchekara, H.R.; Sha'aban, Y.A.; Shahriar, M.S.; Ramli, M.A.; Mas'ud, A.A. Wind Farm Layout Optimization/Expansion with Real Wind Turbines Using a Multi-Objective EA Based on an Enhanced Inverted Generational Distance Metric Combined with the Two-Archive Algorithm 2. *Sustainability* **2023**, *15*, 2525. [CrossRef]
30. Ramli, M.A.; Bouchekara, H.R. Wind Farm Layout Optimization Considering Obstacles Using a Binary Most Valuable Player Algorithm. *IEEE Access* **2020**, *8*, 131553–131564. [CrossRef]
31. Wolpert, D.H.; Macready, W.G. No free lunch theorems for optimization. *IEEE Trans. Evol. Comput.* **2002**, *1*, 67–82. [CrossRef]
32. Chowdhury, S.; Zhang, J.; Messac, A.; Castillo, L. Optimizing the arrangement and the selection of turbines for wind farms subject to varying wind conditions. *Renew. Energy* **2013**, *52*, 273–282. [CrossRef]
33. Cao, L.; Ge, M.; Gao, X.; Du, B.; Li, B.; Huang, Z.; Liu, Y. Wind farm layout optimization to minimize the wake induced turbulence effect on wind turbines. *Appl. Energy* **2022**, *323*, 119599. [CrossRef]
34. Ghamati, E.; Kariman, H.; Hoseinzadeh, S. Experimental and computational fluid dynamic study of water flow and submerged depth effects on a tidal turbine performance. *Water* **2023**, *15*, 2312. [CrossRef]
35. Shakoor, R.; Hassan, M.Y.; Raheem, A.; Wu, Y.K. Wake effect modeling: A review of wind farm layout optimization using Jensen's model. *Renew. Sustain. Energy Rev.* **2016**, *58*, 1048–1059. [CrossRef]
36. Castillo, O.C.; Andrade, V.R.; Rivas, J.J.R.; González, R.O. Comparison of power coefficients in wind turbines considering the tip speed ratio and blade pitch angle. *Energies* **2023**, *16*, 2774. [CrossRef]
37. Biswas, P.P.; Suganthan, P.N.; Amaratunga, G.A. Optimal placement of wind turbines in a windfarm using L-SHADE algorithm. In Proceedings of the 2017 IEEE Congress on Evolutionary Computation (CEC), San Sebastián, Spain, 5–8 June 2017; pp. 83–88.
38. Wang, D.; Tan, D.; Liu, L. Particle swarm optimization algorithm: An overview. *Soft Comput.* **2017**, *22*, 387–408. [CrossRef]
39. Yang, K.; Cho, K. Simulated annealing algorithm for wind farm layout optimization: A benchmark study. *Energies* **2019**, *12*, 4403. [CrossRef]

40. Kennedy, J.; Eberhart, R. Particle swarm optimization. In Proceedings of ICNN'95-International Conference on Neural Networks. In Proceedings of the ICNN'95-International Conference on Neural Networks, Perth, WA, Australia, 27 November–1 December 1995.
41. El-Shorbagy, M.A.; El-Refaey, A.M. A hybrid genetic-firefly algorithm for engineering design problems. *J. Comput. Des. Eng.* **2022**, *9*, 706–730.
42. Haldurai, L.; Madhubala, T.; Rajalakshmi, R. A study on genetic algorithm and its applications. *Int. J. Comput. Sci. Eng.* **2016**, *4*, 139–143.
43. Asaah, P.; Hao, L.; Ji, J. Optimal Placement of Wind Turbines in Wind Farm Layout Using Particle Swarm Optimization. *J. Mod. Power Syst. Clean Energy* **2021**, *9*, 367–375. [CrossRef]

Disclaimer/Publisher's Note: The statements, opinions and data contained in all publications are solely those of the individual author(s) and contributor(s) and not of MDPI and/or the editor(s). MDPI and/or the editor(s) disclaim responsibility for any injury to people or property resulting from any ideas, methods, instructions or products referred to in the content.